ChemPubSoc Europe

DOI: 10.1002/celc.201402312

CHEMELECTROCHEM Communications

Electrochemistry and Electrocatalysis at Single Gold Nanoparticles Attached to Carbon Nanoelectrodes

Yun Yu,[a] Yang Gao,[c] Keke Hu,[a] Pierre-Yves Blanchard,[a] Jean-Marc Noël,[a, e] Thangavel Nareshkumar,[d] Kanala L. Phani,[a, d] Gary Friedman,[c] Yury Gogotsi,*[b] and Michael V. Mirkin*[a]

Electrochemical experiments at individual metal nanoparticles (NPs) can provide new insights into their electrocatalytic behavior. In this Communication, we report the preparation of nanometer-sized carbon electrodes and their use as substrates for the immobilization of single gold NPs (AuNPs). In addition to its very small size, the surface of a carbon nanoelectrode is catalytically inert, which makes it an excellent substrate for studying electrocatalytic reactions. The activity of single AuNPs towards the hydrogen evolution reaction was investigated and compared to that of low-atomicity gold clusters. Three approaches to attaching AuNPs to either chemically modified or bare carbon nanoelectrodes, and the effects of immobilization on hydrogen adsorption and catalytic behavior of AuNPs are discussed. The developed methodology should be useful for studying the effects of NP size, geometry, and surface attachment on the electrocatalytic activity.

Metal nanoparticles (NPs) have attracted a great deal of research interest because of their unique physical and chemical properties. They are extensively utilized as catalysts, owing to their high surface-area-to-mass ratio. Understanding the relationship between the size and structure of a NP and its catalytic activity is essential for fundamental advances in electrocatalysis and technological applications.[1–7] In most published studies, the use of a large ensemble of particles obscures the effects of variations in NP size, shape, orientation, and local environment on the catalytic activity.

Different electrochemical strategies have been proposed to perform experiments at single NPs,[3c] most of which focus on monitoring current transients produced by collisions of a metal particle with a micrometer-sized electrode.[8, 9] Xiao and Bard were the first to detect the landing of catalytic NPs on the microelectrode surface.[8a] Compton and co-workers used the particle collision method to determine the size distribution and concentration of NPs by measuring the charge transferred in the current transient.[10] Such experiments provided information about transport processes and collision dynamics rather than electron transfer (ET) or catalytic reactions.

To access chemical information at a single metal NP, one can attach it to the surface of a nanometer-sized electrode, which has to be sufficiently small to eliminate the possibility of multi-NP binding.[11] In this way, Zhang and co-workers probed the oxygen reduction reaction and the underpotential deposition of Cu at a gold NP (AuNP) attached to the Pt nanoelectrode.[12] This work also showed the importance of using catalytically inert substrate materials in single NP experiments; although well-shaped steady-state voltammograms and chronoamperometric transients were obtained, it was difficult to differentiate between the currents flowing at the AuNP and the underlying Pt surface.

We have previously studied AuNPs attached to glass[13a] and carbon nanopipettes,[13b] but no isolated single particles at the probe tip have been reported. Here, we employ very small carbon nanoelectrodes to measure catalytic currents at a single 10 nm gold particle. To ensure that the electrochemical signal is produced by only one NP, the carbon tip radius (a) must be smaller than, or comparable to, the particle diameter. Such electrodes were prepared by using chemical vapor deposition (CVD) of carbon inside a pre-pulled quartz nanopipette.

Three approaches to the immobilization of AuNPs on the carbon nanoelectrode surface employed in this work are outlined in Scheme 1. The AuNPs may either 1) be directly adsorbed on the carbon surface or 2, 3) be attached through a polyphenylene multilayer film. This film was formed in situ through the electrochemical reduction of the corresponding aryl diazonium compound, as reported previously for macroscopic carbon and metal electrodes.[14] The negatively charged citrate-stabilized AuNP can be electrostatically attached to the positive polyphenylene layer (2). Even stronger AuNP binding was attained by converting terminal amine groups to diazoni-

[a] Y. Yu, K. Hu, Dr. P.-Y. Blanchard, Dr. J.-M. Noël, Dr. K. L. Phani, Prof. M. V. Mirkin
Department of Chemistry and Biochemistry
Queens College - The City University of New York
65-30 Kissena Blvd., Flushing, NY 11367 (USA)
E-mail: mmirkin@qc.cuny.edu

[b] Prof. Y. Gogotsi
Department of Materials Science and Engineering
and A. J. Drexel Nanomaterials Institute, Drexel University
3141 Chestnut St., Philadelphia, PA 19104 (USA)
E-mail: gogotsi@drexel.edu

[c] Y. Gao, Prof. G. Friedman
Department of Electrical and Computer Engineering
3141 Chestnut St., Philadelphia, PA 19104 (USA)

[d] T. Nareshkumar, Dr. K. L. Phani
Electrodics and Electrocatalysis Division
CSIR-Central Electrochemical Research Institute
Karaikudi, India - 630 006 (India)

[e] Dr. J.-M. Noël
Paris Diderot, Sorbonne Paris Cité, ITODYS, UMR 7086 CNRS
15 rue J-A de Baïf, 75205 Paris Cedex 13 (France)

Supporting Information for this article is available on the WWW under http://dx.doi.org/10.1002/celc.201402312.

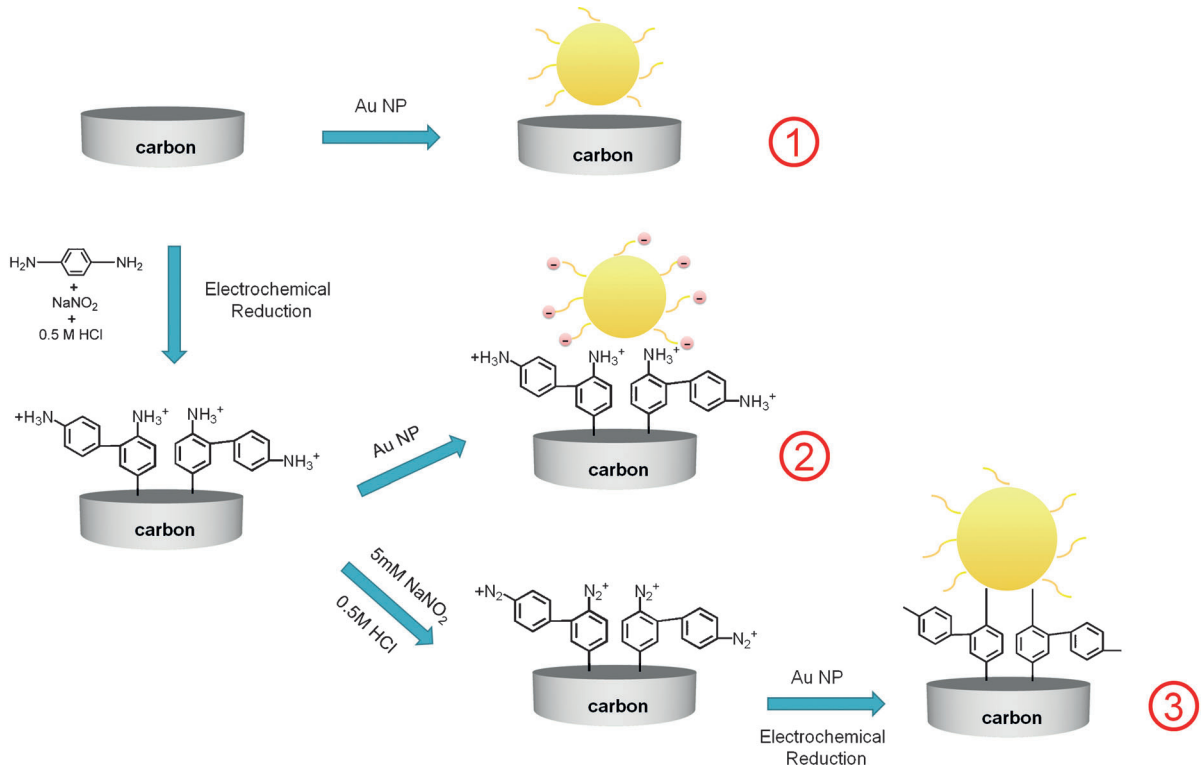

Scheme 1. Schematic representation of the three methods of AuNP immobilization on a carbon nanoelectrode.

um and subsequent electrochemical reduction, resulting in C–Au covalent bonding (3); this methodology was developed by Liu et al. for modifying macroscopic carbon electrodes.[15]

A transmission electron microscopy (TEM) image of the tip of the pulled quartz nanopipette completely filled with carbon is shown in Figure 1 A. Although CVD was conducted at 900 °C, which is significantly lower than the strain temperature of quartz capillaries (>1000 °C), the tip of a very small (e.g. <20 nm) pipette typically melted, and the deposited carbon was completely encased in quartz (Figure 1 A). When used as a working electrode, such insulated pipettes produced no electrochemical signal until the carbon surface was exposed by polishing. A TEM image of a 20 nm AuNP directly attached to the carbon nanoelectrode is shown in Figure 1 B.

Curve 1 in Figure 2 A is a voltammogram of ferrocenemethanol (FcMeOH) obtained at a polished carbon nanoelectrode. From the diffusion-limiting steady-state current, the effective

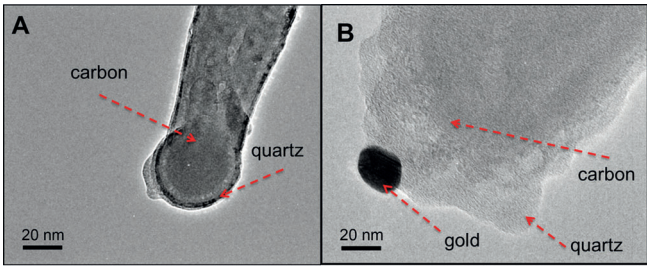

Figure 1. TEM images of A) a pulled quartz nanopipette filled with carbon by CVD and B) a carbon nanoelectrode with a 20 nm AuNP attached to its tip.

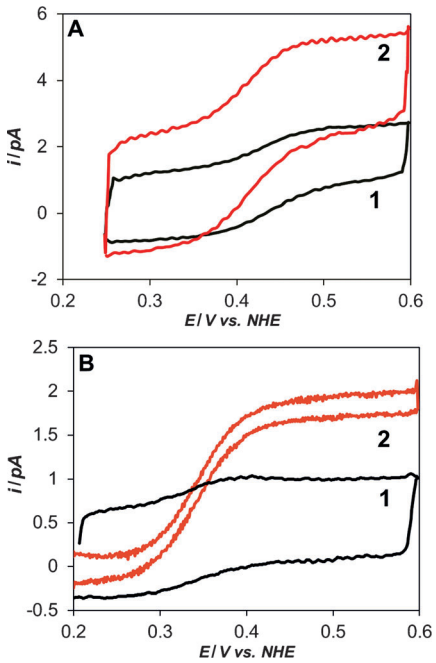

Figure 2. Steady-state voltammograms of 1 mM FcMeOH in 0.2 M KCl obtained at carbon nanoelectrodes before (1) and after (2) attaching a 10 nm AuNP. The AuNP was attached to A) the bare carbon surface and B) the carbon electrode modified with a polyphenylene film. Potential sweep rate, $v = 50\ mV\ s^{-1}$.

radius, $a = 3$ nm, can be evaluated by using Equation (1) for the inlaid disk:

$$i_d = 4nFDc^*a \quad (1)$$

where $n=1$ is the number of electrons transferred, F is the Faraday constant, $c^*=1$ mM and $D=7.6\times10^{-6}$ cm^2 s^{-1}[16] are the bulk concentration and the diffusion coefficient of FcMeOH, respectively. After this electrode spent 2 h in a solution (ca. 9 nM) of 10 nm AuNPs, the diffusion-limiting current increased to approximately 3.2 pA, which is the value that is expected for a 10 nm diameter spherical electrode (curve 2). Although the mechanism of the NP attachment to the bare carbon surface is not completely clear, the electrode response was stable and reproducible on the time scale of hours. A similar behavior has previously been observed at macroscopic glassy carbon electrodes.[17]

An AuNP can also be attached to the carbon electrode by modifying its surface with a multilayer polyphenylene film produced by the electrochemical reduction of the corresponding aryl diazonium compound (see the Supporting Information for details).[14] In Figure 2B, the effective radius of the carbon electrode extracted from curve 1 was ≈1 nm. The diffusion-limiting current in curve 2, recorded after the reduction of aryl diazonium at this electrode and subsequent attachment of a AuNP, was somewhat smaller than that in Figure 2A, because the NP was partially buried in the polyphenylene layer.[14b]

The increased current of FcMeOH oxidation provides evidence for efficient ET between the AuNP and the carbon nanoelectrode. Previous studies at macroscopic electrodes showed that a polyphenylene multilayer film with a thickness as large as 20 nm does not strongly block ET between the immobilized NPs and the underlying electrode surface.[14b] One reason is that the NPs are buried inside the layer. Also, efficient ET between the electrode and metal NPs across relatively thick (several nanometer) insulating films has been observed experimentally[18a,b] and elucidated theoretically.[18c]

The catalytic effect of the NPs can be seen by comparing voltammograms of the hydrogen evolution reaction (HER) from 0.1 M $HClO_4$ obtained at a bare carbon nanoelectrode (curve 1 in Figures 3A and 3B) to those recorded after attaching a AuNP to its surface (curve 2 in Figures 3A and 3B). A significant (>0.5 V) shift in the current onset potential corresponds to the much higher activity of the AuNP towards proton reduction. The HER onset at the AuNP directly sticking to the carbon surface (Figure 3A) occurs at significantly more positive potentials than at those attached through the polyphenylene film (Figure 3B). This difference can probably be attributed to the insulating properties of the film, which impede ET between the carbon surface and the AuNP.

Figure 3D shows the Tafel plot for the HER, obtained from the polarization curve of Figure 3A. The linear portion at higher overpotentials exhibits a 0.12 V dec^{-1} slope, consistent with literature data for the HER at polycrystalline Au.[19] However, a smaller Tafel slope (ca. 0.03 V dec^{-1}) at lower overpotential was not observed, probably because of the passivating effect of the citrate stabilizer.

Carbon nanoelectrodes can also be used to probe the catalytic activity of low-atomicity gold clusters,[20] (Au_x, $2<x<13$, with Au_5 being the principal species;[21] see the Supporting Information). Very small Au clusters can act as active chemical catalysts[20b] and electrocatalysts,[20c,21,22] thus representing an intriguing intermediate case between molecular and heterogeneous catalysis. The effect of modifying the carbon nanoelectrode surface with Au clusters on the HER is shown in Figure 3C. Although addressing a single metal atomic cluster was not feasible by using our current experimental setup, catalytically inert carbon nanoelectrodes with extremely low background currents and wide potential windows can facilitate the study of electrocatalysis at such species. In Figure 3C, the current onset of the HER at atomic Au clusters occurs at significantly less-negative potentials than at 10 nm AuNPs. The disordered nature of the cetyltrimethyl ammonium bromide (CTAB) protecting layers on Au clusters is likely to expose catalytically active edge or defect sites and enhance the catalytic activity of Au clusters.[21] One should notice that the adsorption of atomic gold clusters does not appreciably change the diffusion current of FcMeOH to a carbon nanoelectrode as small as 15 nm radius (Figure S4). This is attributed to the sub-nanometer size

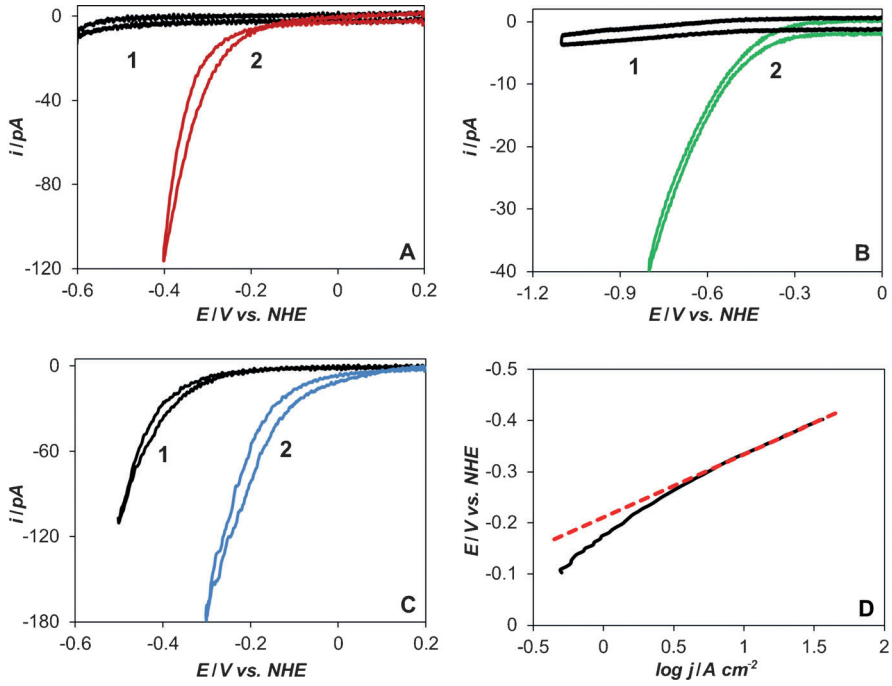

Figure 3. Voltammograms of the HER from 0.1 M $HClO_4$ at a carbon nanoelectrode (1), single AuNP attached to it either directly (curve 2 in A) or through a polyphenylene film (curve 2 in B), and Au_x clusters (curve 2 in C). $a=3$ (A), 1 (B), and 8 nm (C). $v=100$ mV s^{-1}. Tafel plot (D) for the HER obtained from curve 2 in (A).

of the clusters, which, unlike AuNPs, do not significantly increase the geometric surface area of the electrode (cf. Figure S4 and Figure 2).

The inert carbon surface is a convenient substrate for investigating hydrogen adsorption at AuNPs. Brust and Gordillo[23] recently reported hydrogen adsorption peaks at 1–16 nm AuNPs immobilized on a mercury surface. No such peaks have been observed at macroscopic gold electrodes. In Figure 4,

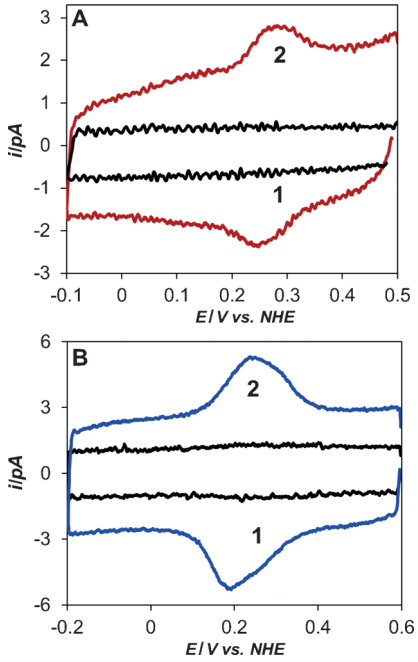

Figure 4. Voltammograms of hydrogen adsorption/desorption obtained at carbon nanoelectrodes in 0.1 M $HClO_4$ before (1) and after (2) the attachment of AuNPs. The AuNPs were attached to the carbon surface A) covalently and B) electrostatically.

a pair of adsorption/desorption peaks can be seen at carbon nanoelectrodes with 10 nm AuNPs immobilized (curve 2), but not at the same electrodes before the attachment of the particles (curve 1). The current produced by hydrogen adsorption at a single 10 nm Au NP is too low to measure with our experimental setup; therefore, the voltammograms in Figure 4 were obtained with a number of AuNPs attached to larger ($a \geq$ 100 nm) carbon nanoelectrodes. The linear dependence of the peak current on the potential sweep rate (Figures S5A and S5B) indicates that the electroactive species is adsorbed on the electrode surface.

The effect of AuNP immobilization on hydrogen adsorption was investigated by using different procedures to attach the NPs to the carbon nanoelectrodes (Scheme 1). Figure 4A shows a cyclic voltammogram of hydrogen adsorption/desorption at AuNPs covalently attached to the surface by generating diazonium radicals at the polyphenylene layer, which resulted in covalent-bond formation between the film and the NPs[15] (attachment method 3 in Scheme 1). The half-peak width ($\Delta E_{p/2}$), which is expected to be 90.6/n mV for a n-electron Nernstian oxidation/reduction involving adsorbed species,[24] is close to 45 mV in Figure 4A and to 90 mV in Figure 4B obtained with AuNPs electrostatically attached to the polyphenylene film (attachment method 2 in Scheme 1). This result, which has been reproduced by using several carbon nanoelectrodes, suggests different numbers of transferred electrons for hydrogen adsorption occurring at the covalently ($n=2$) attached AuNPs compared to the electrostatically ($n=1$) attached AuNPs. The former number was found in Ref. [23] and interpreted as the predominance of the reductive proton adsorption followed by reduction of the second proton at the same site (Volmer–Heyrovsky mechanism). Our data also agrees with the suggestion that neither the use of Hg as the substrate for AuNP attachment nor the thiol protection of the particles was essential for observing the hydrogen adsorption/desorption peaks.[23] The slope of the linear peak potential E_p versus pH dependence is shown in Figure S5C to be 57 mV per pH unit, which is very similar to the 58 mV per pH unit slope measured in Ref. [23] at the ensemble of AuNPs pre-adsorbed on mercury.

The $\Delta E_{p/2} \approx 100$ mV in Figure 4B suggests a one-electron-transfer process attributable to the Volmer–Tafel mechanism. Although additional data is required to explain the difference in catalytic responses of covalently and electrostatically attached NPs, possible reasons include changes in the protective layer of AuNPs and the extent of their aggregation. Specifically, it was shown that the citrate protective layer desorbs from the AuNPs at negative potentials applied to effect the covalent immobilization of AuNPs.[15] The removal of stabilizing ligands may have increased the number of active sites, facilitating the one-electron reduction followed by recombination of adsorbed atomic hydrogen. Another possible factor is that the effective NP potential seen by the solution species may depend on the immobilization method.

In summary, we used carbon nanoelectrodes with a well-defined geometry to investigate the catalytic responses of single AuNPs and atomic gold clusters. Three different methods were used for attaching NPs to the electrode surface, which showed significant effects of the particle immobilization on HER catalysis and hydrogen adsorption. The electrostatic attachment of a AuNP to the polyphenylene film used as an anchoring layer resulted in a less efficient HER catalysis, as compared to that at a similar NP adsorbed directly on the carbon surface. Different effective numbers of transferred electrons were found for hydrogen adsorption on covalently and electrostatically attached AuNPs. The developed methodology should be useful for studying the effects of NP size and geometry on the electrocatalytic activity.[25]

Experimental Section

Fabrication of Carbon Nanoelectrodes

Nanopipettes with tip diameters from 10 to 100 nm were pulled by a laser pipette puller (P-2000; Sutter Instruments) from quartz capillaries (outer diameter, OD = 1.0 mm, internal diameter, ID =

0.3 mm, or OD = 1.0 mm, ID = 0.7 mm; Sutter Instruments). Carbon was deposited inside the pulled quartz pipette by CVD, using methane as the carbon source and argon (Ar) as the protector, as described previously.[26] The Ar flow of 200 sccm (standard cubic centimeters per minute) was passed through the CVD reaction chamber during heating. Once the furnace temperature reached 875 °C, a mixed flow of methane and Ar was passed through the reaction chamber. The thickness and distribution of the carbon layer depended on the pipette shape, the tip diameter, the CVD time, and the composition of the gas mixture. For the quartz nanopipettes used in this work, the CVD time of 3 h and the 1:1 methane-to-Ar ratio normally produced nanoelectrodes with the pipette orifice completely filled with carbon. Several other factors, including the furnace temperature and total gas flow rate, can also affect the synthesized carbon layer morphology. To expose the carbon surface, the electrodes were polished under video microscopic control, as described previously.[16] Briefly, a micromanipulator was used to move the nanoelectrode towards the slowly rotating disk covered with 50 nm lapping tape. The video microscope was used to roughly evaluate the distance between the tip and the lapping tape and to ensure that the tip never touches the polishing disk to avoid a significant increase in its radius.

Immobilization of AuNPs and Au Clusters on Carbon Nanoelectrodes

AuNPs were either directly attached (adsorbed) on the carbon surface, electrostatically attached to the polyphenylene film, or covalently linked through the reduction of an aryl diazonium salt. In the first case, a carbon nanoelectrode was immersed in AuNP solution for 1.5–2 h, and a single AuNP spontaneously attached to its tip, as confirmed by using voltammetry and TEM (Figures 1 B and 2 A). A polyphenylene multilayer (C–Ph–NH_2) resulted from the reduction of the corresponding aryl diazonium compound on the carbon nanoelectrode by applying to it one triangular potential sweep between 0.1 V and −0.8 V versus Ag/AgCl. Aryl diazonium was formed in situ by mixing 50 mM $NaNO_2$ (200 μL) with aqueous solution containing 10 mM *p*-phenylenediamine and 0.5 M HCl (1 mL).[14] The modified nanoelectrode was kept in 0.1 M HCl for 10 s to protonate $-NH_2$ to $-NH_3^+$. The negatively charged citrate-stabilized AuNPs were electrostatically attached to the protonated film by immersing the electrode in AuNP solution for 2 h. For the covalent attachment, the C–Ph–NH_2 surface was first immersed in 5 mM $NaNO_2$ and 0.5 M HCl for 15 min followed by two potential cycles between 0.1 V and −0.8 V versus Ag/AgCl in AuNP solution at a scan rate of 100 mV s^{-1}.[15] To attach Au_x clusters to a carbon nanoelectrode, the clusters electrodeposited on a gold foil (see the Supporting Information) were dispersed in a dilute aqueous CTAB solution. The carbon electrode was kept in this dispersion for approximately 30 min and then thoroughly rinsed with a water jet to remove unattached clusters.

Acknowledgements

We thank Pansy Elsamadisi for assistance with nanoelectrode polishing. This work was supported by the National Science Foundation (CHE-1026582) and Air Force Office of Scientific Research (AFOSR) Multi-university Research Initiative (MURI) (FA9550–14–1–0003). K.L.P. thanks United States–India Educational Foundation (USIEF) for the award of Fulbright-Nehru Senior Research Fellowship (2012–13).

Keywords: electrocatalysis · hydrogen evolution reaction · nanoelectrochemistry · nanoelectrodes · nanoparticles

[1] a) R. W. Murray, *Chem. Rev.* **2008**, *108*, 2688–2720; b) A. Wieckowski, E. R. Savinova, C. G. Vayenas, *Catalysis and Electrocatalysis at Nanoparticle Surfaces*, Marcel Dekker, New York, **2003**.
[2] a) X. Shan, I. Diez-Perez, L. Wang, P. Wiktor, Y. Gu, L. Zhang, W. Wang, J. Lu, S. Wang, Q. Gong, J. Li, N. Tao, *Nat. Nanotechnol.* **2012**, *7*, 668–672; b) W. Wang, N. Tao, *Anal. Chem.* **2014**, *86*, 2–14.
[3] a) S. C. S. Lai, P. V. Dudin, J. V. Macpherson, P. R. Unwin, *J. Am. Chem. Soc.* **2011**, *133*, 10744–10747; b) S. E. F. Kleijn, S. C. S. Lai, T. S. Miller, A. I. Yanson, M. T. M. Koper, P. R. Unwin, *J. Am. Chem. Soc.* **2012**, *134*, 18558–18561; c) S. E. Kleijn, S. C. Lai, M. T. Koper, P. R. Unwin, *Angew. Chem. Int. Ed.* **2014**, *53*, 3558–3586.
[4] K. Yamamoto, T. Imaoka, W.-J. Chun, O. Enoki, H. Katoh, M. Takenaga, A. Sonoi, *Nat. Chem.* **2009**, *1*, 397–402.
[5] M. Shao, A. Peles, K. Shoemaker, *Nano Lett.* **2011**, *11*, 3714–3719.
[6] M. Nesselberger, M. Roefzaad, R. Fayçal Hamou, P. U. Biedermann, F. F. Schweinberger, S. Kunz, K. Schloegl, G. K. H. Wiberg, S. Ashton, U. Heiz, K. J. J. Mayrhofer, M. Arenz, *Nat. Mater.* **2013**, *12*, 919–924.
[7] C. M. Sánchez-Sánchez, J. Solla-Gullón, F. J. Vidal-Iglesias, A. Aldaz, V. Montiel, E. Herrero, *J. Am. Chem. Soc.* **2010**, *132*, 5622–5624.
[8] a) X. Xiao, A. J. Bard, *J. Am. Chem. Soc.* **2007**, *129*, 9610–9612; b) X. Xiao, F.-R. F. Fan, J. Zhou, A. J. Bard, *J. Am. Chem. Soc.* **2008**, *130*, 16669–16677; c) S. J. Kwon, H. Zhou, F.-R. F. Fan, V. Vorobyev, B. Zhang, A. J. Bard, *Phys. Chem. Chem. Phys.* **2011**, *13*, 5394–5402; d) S. J. Kwon, A. J. Bard, *J. Am. Chem. Soc.* **2012**, *134*, 7102–7108; e) H. Zhou, J. H. Park, F.-R. F. Fan, A. J. Bard, *J. Am. Chem. Soc.* **2012**, *134*, 13212–13215.
[9] a) R. Dasari, D. A. Robinson, K. J. Stevenson, *J. Am. Chem. Soc.* **2013**, *135*, 570–573; b) R. Dasari, B. Walther, D. A. Robinson, K. J. Stevenson, *Langmuir* **2013**, *29*, 15100–15106.
[10] a) N. V. Rees, Y.-G. Zhou, R. G. Compton, *ChemPhysChem* **2011**, *12*, 1645–1647; b) Y.-G. Zhou, N. V. Rees, R. G. Compton, *Angew. Chem. Int. Ed.* **2011**, *50*, 4219–4221; *Angew. Chem.* **2011**, *123*, 4305–4307.
[11] S. Chen, A. Kucernak, *J. Phys. Chem. B* **2003**, *107*, 8392–8402.
[12] Y. Li, J. T. Cox, B. Zhang, *J. Am. Chem. Soc.* **2010**, *132*, 3047–3054.
[13] a) E. A. Vitol, Z. Orynbayeva, M. J. Bouchard, J. Azizkhan-Clifford, G. Friedman, Y. Gogotsi, *ACS Nano* **2009**, *3*, 3529–3536; b) S. Bhattacharyya, D. Staack, E. A. Vitol, R. Singhal, A. Fridman, G. Friedman, Y. Gogotsi, *Adv. Mater.* **2009**, *21*, 4039–4044.
[14] a) D. Bélanger, J. Pinson, *Chem. Soc. Rev.* **2011**, *40*, 3995–4048; b) J.-M. Noël, D. Zigah, J. Simonet, P. Hapiot, *Langmuir* **2010**, *26*, 7638–7643; c) H. L. n. Gehan, L. Fillaud, N. Felidj, J. Aubard, P. Lang, M. M. Chehimi, C. Mangeney, *Langmuir* **2010**, *26*, 3975–3980; d) J. Lyskawa, D. Bélanger, *Chem. Mater.* **2006**, *18*, 4755–4763.
[15] G. Liu, E. Luais, J. J. Gooding, *Langmuir* **2011**, *27*, 4176–4183.
[16] P. Sun, M. V. Mirkin, *Anal. Chem.* **2006**, *78*, 6526–6534.
[17] A. J. Wain, *Electrochim. Acta* **2013**, *92*, 383–391.
[18] a) J. Zhao, C. R. Bradbury, S. Huclova, I. Potapova, M. Carrara, D. J. Fermín, *J. Phys. Chem. B* **2005**, *109*, 22985–22994; b) J. Kim, B.-K. Kim, S. K. Cho, A. J. Bard, *J. Am. Chem. Soc.* **2014**, *136*, 8173–8176; c) J.-N. Chazalviel, P. Allongue, *J. Am. Chem. Soc.* **2011**, *133*, 762–764.
[19] J. Perez, E. R. Gonzalez, H. M. Villullas, *J. Phys. Chem. B* **1998**, *102*, 10931–10935.
[20] a) M. J. Rodríguez-Vázquez, M. C. Blanco, R. Lourido, C. Vázquez-Vázquez, E. Pastor, G. A. Planes, J. Rivas, M. A. López-Quintela, *Langmuir* **2008**, *24*, 12690–12694; b) J. Oliver-Meseguer, J. R. Cabrero-Antonino, I. Domínguez, A. Leyva-Pérez, A. Corma, *Science* **2012**, *338*, 1452–1455; c) A. Corma, P. Concepción, M. Boronat, M. J. Sabater, J. Navas, M. J. Yacaman, E. Larios, A. Posadas, M. A. López-Quintela, D. Buceta, E. Mendoza, G. Guilera, A. Mayoral, *Nat. Chem.* **2013**, *5*, 775–781.
[21] C. Jeyabharathi, S. Senthil Kumar, G. V. M. Kiruthika, K. L. N. Phani, *Angew. Chem. Int. Ed.* **2010**, *49*, 2925–2928; *Angew. Chem.* **2010**, *122*, 2987–2990.
[22] W. Chen, S. Chen, *Angew. Chem. Int. Ed.* **2009**, *48*, 4386–4389; *Angew. Chem.* **2009**, *121*, 4450–4453.
[23] M. Brust, G. J. Gordillo, *J. Am. Chem. Soc.* **2012**, *134*, 3318–3321.
[24] A. J. Bard, L. R. Faulkner, *Electrochemical Methods: Fundamentals and Applications*, John Wiley & Sons, Inc., New York, **2001**, Chapter 14.

[25] J. Solla-Gullón, F. J. Vidal-Iglesias, J. M. Feliu, *Annu. Rep. Prog. Chem. C* **2011**, *107*, 263 – 297.
[26] a) R. Singhal, S. Bhattacharyya, Z. Orynbayeva, E. Vitol, G. Friedman, Y. Gogotsi, *Nanotechnology* **2010**, *21*, 015304; b) E. A. Vitol, M. G. Schrlau, S. Bhattacharyya, P. Ducheyne, H. H. Bau, G. Friedman, Y. Gogotsi, *Chem. Vap. Deposition* **2009**, *15*, 204 – 208; c) Y. Yu, J.-M. Noël, M. V. Mirkin, Y. Gao, O. Mashtalir, G. Friedman, Y. Gogotsi, *Anal. Chem.* **2014**, *86*, 3365 – 3372.

Received: September 12, 2014
Published online on October 8, 2014